Effect of Unsaturated Lipid Chains on Dimensions, Molecular Order and Hydration of Membranes

ARTICLE *in* THE JOURNAL OF PHYSICAL CHEMISTRY B · DECEMBER 2001

Impact Factor: 3.3 · DOI: 10.1021/jp010118h

Effect of Unsaturated Lipid Chains on Dimensions, Molecular Order and Hydration of Membranes

Hans Binder*,† and Klaus Gawrisch‡

University of Leipzig, Institute of Medical Physics and Biophysics, Liebigstr. 27, D-04103 Leipzig, Germany, and NIH, NIAAA, Laboratory of Membrane Biochemistry and Biophysics, 12420 Parklawn Drive, Rockville, Maryland 20852

Received: December 31, 2000; In Final Form: August 23, 2001

We conducted infrared linear dichroism and X-ray measurements to characterize membranes of sn-1 chain perdeuterated, polyunsaturated 1-stearoyl-2-docosahexaenoyl-sn-glycero-3-phosphocholine (18:0−22:6ω3 PC, SDPC-d35) and of monounsaturated 1-palmitoyl-2-oleoyl-sn-glycero-3-phosphocholine (16:0−18:1 PC, POPC-d31) as a function of hydration and temperature. Our novel approach is to use IR order parameters of C−H and C−D vibrations of both sn-1 and sn-2 chains for a separate estimation of the mean length and effective cross sectional area of the saturated and unsaturated chains in the bilayers. In the gel phase, the thickness of the hydrophobic core of SDPC bilayers exceeded the thickness of POPC bilayers, because the polyunsaturated chains adopted an extended conformation. However, in the fluid phase, the hydrophobic thickness of SDPC membranes, with the longer 18:0 and 22:6 acyl chains, was almost equal to the thickness of the 16:0−18:1 chains in POPC membranes. The isothermal compressibility modulus of the docosahexaenoyl chains was smaller than the modulus of the stearoyl chains of SDPC, whereas the palmitoyl and oleoyl chains of POPC are similarly compressible. Analysis in terms of a simple polymer brush model showed that unsaturation increases chain flexibility and chain mean area in lipid membranes. Temperature dependent measurements indicated that polyunsaturation decreased the sensitivity of the bilayer to temperature changes. The study of lipid hydration-sensitive spectral parameters suggested that this tendency may be at least partially explained by a weakening of water binding to polar moieties of polyunsaturated lipids with increasing temperature. Although the influence of hydrocarbon chain polyunsaturation on hydration of phosphate groups and the entire lipid was minor, we observed a modification of lipid carbonyl group hydration. Hydration properties and phase behavior of SDPC suggest an influence from polyunsaturation on the lateral pressure profile across the bilayer.

Introduction

The meta I to meta II transition in rhodopsin is eased by the presence of docosahexaenoyl (DHA, 22:6ω3) acyl chains. In particular, near-native levels of 50% of DHA, as in retinal rod outer segment disk membranes, are required for proper function of the visual receptor.[1,2] The model of rhodopsin activation is linked to a sequence of transient deformations and tilt of the transmembrane α-helices forming the protein. This cascade of structural rearrangements propagates from the retinal binding site at the center of the transmembrane helices to the loops at the membrane surface that bind the G-protein transducin.[3] Various transport proteins such as the Ca-ATPase, a calcium pump active in muscle contraction, the ubiquitous transporters that control the levels of neurotransmitter substances in the brain, and the G-protein-coupled drug receptors all seem to undergo similar conformational changes as part of their molecular mechanism of action. Recent investigations provide direct evidence that DHA-containing lipids may facilitate a conformational change of another transmembrane protein, the class I major histocompatibility complex (MHC I). By modulating MHC I function, the polyunsaturated lipid alters the activation of T-cells and the outcome of immune responses.[4] The general question arises how polyunsaturated lipids affect protein function.

At present, the physical mechanisms by which lipids influence membrane-embedded proteins are not well understood. Systematic investigations of the dependence of membrane protein function on the lipid bilayer composition show that chemical specificity is of little importance for most protein−lipid interactions.[5,6] On the contrary, changes in membrane protein function can be correlated with changes in the bilayer material properties such as bilayer hydrophobic thickness[7−9] and monolayer curvature stress.[10,11]

Theoretical considerations showed that the lateral pressure and its profile through the membrane may serve as another essential property for those intrinsic proteins whose function involves a conformational change accompanied by a depth-dependent variation in the cross-sectional area of the protein, because relatively small modifications of the lateral pressure profile can induce considerable shifts of the equilibrium between different protein conformers.[12] Variation in the degree and position of unsaturation induces changes in the transverse pressure profile of lipid bilayers.[13] At the same time, polyunsaturation shortens effective chain length because of increased segmental disorder. Hence, more chain segments are necessary

* To whom correspondence should be addressed. E-mail: binder@rz.uni-leipzig.de. Fax: +49-341-9715709.
† Institute of Medical Physics and Biophysics.
‡ NIH, NIAAA, Laboratory of Membrane Biochemistry and Biophysics.

10.1021/jp010118h CCC: $20.00
Published on Web 11/13/2001

to maintain bilayer thickness. These theoretical predictions encouraged us to test the relation between bilayer dimensions, chain ordering, and the pressure acting within membranes of unsaturated lipids.

Hydration-dependent deformation of multibilayer assemblies is a well-established method in lipid research.[14,15] This so-called osmotic stress technique is capable of probing compressibility of bilayer stacks in the directions perpendicular and parallel to the membrane surface.[16−19] Here we applied this method in combination with infrared (IR) linear dichroism and X-ray measurements to study the effect of hydration on membranes of polyunsaturated 1-stearoyl-2-docosahexaenoyl-sn-glycero-3-phosphocholine (SDPC-d35) and compared it with membranes of monounsaturated 1-palmitoyl-2-oleoyl-sn-glycero-3-phosphocholine (POPC-d31). This publication continues previous work on lyotropic phase behavior of SDPC.[20] A new fluid lamellar phase (L_α') was found in partially hydrated samples at $T > 15$ °C. Interestingly, L_α' membranes expanded laterally when water was removed. This indicates an unusual interaction between SDPC molecules in membranes. The saturated and monounsaturated PCs usually contract laterally or bend into nonlamellar structures upon dehydration.

From a methodological point of view, the novelty in this study is to use IR order parameters of C−H and C−D vibrations of the sn-1 and sn-2 chains to estimate the effective dimensions of the saturated and unsaturated chains as a function of compression. In addition, vibrations of the carbonyl and phosphate groups provide information on local hydration properties that depend on the local pressure acting within the polar membrane region. In the first part we outline the theoretical background of the method. In the second part we analyze and discuss experimental data that were partially taken from our previous publication.[20]

Experimental Section

Materials. The lipids 1-stearoyl-2-docosahexaenoyl-sn-glycero-3-phosphocholine (SDPC) and 1-palmitoyl-2-oleoyl-sn-glycero-3-phosphocholine (POPC) and their perdeuterated analogues (SDPC-d35 and POPC-d31) were purchased from Avanti Polar Lipids, Inc. (Alabaster, AL). The stearic acid chain is about 98% deuterated,[21] except for the C2 methylene segment that is deuterated to about 50% only. The lipids were stored as methylene chloride stock solutions with butylated hydroxy toluene (BHT-to-lipid mole/mole 1:250) to minimize oxidation. Lipid purity was checked by matrix-assisted laser desorption and ionization time-of-flight mass spectrometry (MALDI-TOF-MS) which detects lipid peroxidation products with high sensitivity.[22]

Infrared Measurements and Spectral Analysis. Samples were prepared by spreading appropriate amounts of the stock solution of lipid in methylene chloride on the surface of a ZnSe-attenuated total reflection (ATR) crystal. The solvent evaporated under a stream of nitrogen in less than one minute. The average thickness of the lipid film was less than 3 μm, corresponding to a stack of about 500 bilayers. The molecular properties of the macroscopically oriented multibilayer films appear to be not influenced by the underlying solid surface. The phase behavior of dipalmitoylphosphatidylcholine (DPPC) oriented bilayers that have been prepared in the same fashion completely agrees with that of bulk samples.[23] Diffraction experiments on solid-supported lipid films containing ~1800 bilayers resulted in repeat spacings similar to those of unoriented multilamellar liposomes.[24] Calorimetric and NMR measurements show that a solid support influences only the bilayers that are in immediate contact with the solid surface.[25]

After application of the lipid, the ATR crystal was immediately mounted inside a sample chamber.[26] The sample chamber was placed into a BioRad FTS-60a Fourier transform infrared spectrometer (Digilab, MA) equipped with a wire grid polarizer. The lipid films were hydrated in a stream of high purity nitrogen gas at definite relative humidity (RH) which was led through the sample chamber. The temperature (T) and RH were adjusted by means of a water-circulating thermostat (Julabo, Seelbach, Germany) and a moisture generator (Humi-Var, Leipzig, Germany) with an accuracy of ±0.1 K and ±0.5%, respectively. Hydration/dehydration scans were performed by increasing/decreasing RH in steps of $\Delta RH = 3\%$ in the range 5−98% at constant T. Heating/cooling scans were performed by increasing/decreasing T in steps of $\Delta T = 1$ K at RH = const. The sample was allowed to equilibrate for 10 min in RH scans and for 2 min in temperature scans before the measurement. No significant hysteresis effects were detected. In addition to hydration studies using H_2O, the measurements were conducted in a D_2O atmosphere to improve the resolution in the spectral regions of the CH_2 and C═O stretches which overlap with the H_2O stretching and bending bands, respectively.

Polarized absorption spectra, $A_{||}(\nu)$ and $A_\perp(\nu)$, were recorded with light polarized parallel and perpendicular with respect to the plane of incidence (128 accumulations each). Band positions were analyzed by means of their center of gravity (COG) in the weighted sum spectrum, $A(\nu) = A_{||}(\nu) + K_2A_\perp(\nu)$.[27] Integral baseline-corrected intensities of selected absorption bands were used to calculate the dichroic ratio, $R_{ATR} = A_{||}/A_\perp$, and the respective IR order parameter, S_{IR}, that was calculated at $K_1 = 2$ and $K_2 = 2.55$ (see the Theory section, eqs 2 and 5).

X-Ray Measurements. For X-ray investigations, oriented multibilayer stacks of the lipids were prepared by spreading appropriate amounts of the stock solution on glass slides (20 × 25 mm). Subsequently, the organic solvent was evaporated. The slides were positioned into a sealed thermostated (±0.5 K) chamber mounted at a conventional Philips PW3020 powder diffractometer (Philips, Netherlands). X-ray diffractograms were obtained with Ni-filtered Cu Kα radiation (20 mA/30 kV) by $\Theta_{X-ray}/2\Theta_{X-ray}$ scans. The intensity was detected with a proportional detector system. Nitrogen of definite RH was continuously streamed through the sample chamber using a moisture-regulating unit (see above). The samples were investigated at discrete RH values and equilibrated for at least 1 h before measurements. Repeat distances of the lamellar phase, d, were determined with an accuracy of ±0.1 nm using the Bragg peaks of up to fourth order. Original X-ray data of SDPC were published previously.[20]

Theory

Infrared Order Parameter. Let us first consider absorption of a single IR active group in the ATR experiment. Its integral polarized IR absorbances are[27]

$$A_{||}^{\,i} = C^i(K_1^{\,i} + K_2^{\,i}S_{IR}^{\,i})\epsilon^i \quad \text{and} \quad A_\perp^{\,i} = C^i(1 - S_{IR}^{\,i})\epsilon^i \quad (1)$$

where ϵ^i is the integral absorption coefficient of group i and $C^i = (3n_{21}/2 \cos \omega)(E_{y'}(d^i)/E_0)^2$ denotes a constant that depends (i) on the ratio of the refractive indices of the sample and the ATR crystal ($n_{21} = n_{sample}/n_{ATR}$), (ii) on the angle of incidence ($\omega = 45°$), (iii) on the distance of the group from the ATR surface, d^i, (iv) on the electric field amplitude of the incident light, E_0, and (v) on the electric field component pointing perpendicular to the plane of incidence at the position of the absorbing group, $E_{y'}(d^i)$. The optical constants $K_1^{\,i} \equiv (E_{z'}/E_{y'})^2$

$+ (E_{x'}/E_{y'})^2$ and $K_2^i \equiv 2(E_{z'}/E_{y'})^2 - (E_{x'}/E_{y'})^2$ depend on the Cartesian coordinates of the normalized electric field vector (with z′ oriented perpendicular to the ATR surface) which interact with the IR active transition moment μ^i of the investigated molecular group. The IR order parameter of the considered absorption band, $S_{IR}^i \equiv P_2(\theta_\mu^i)$, is defined as the second-order Legendre polynomial, $P_2(\theta_\mu^i) \equiv 0.5(3\cos^2\theta_\mu^i - 1)$, of the angle θ_μ^i between μ^i and the ATR normal, **n**.

In a next step of approximation we consider a molecule (e.g., a lipid) that contains n_{group} absorbing groups of the same type (e.g., methylenes) that may differ in orientation and absorption coefficients. Moreover, we proceed to a sample film of thickness d_{film} on an ATR crystal with N_{ref} active reflections. The electric field amplitudes, and thus the optical constants, are conveniently obtained in terms of *Harricks* thick-film approximation (which is valid for the used ZnSe crystal at $d_{film} > 0.2\lambda$, where λ is the wavelength of absorbed light) using *Fresnels* equations:[29]

$$K_1 = \frac{2\sin^2\omega - n_{21}^2}{(1+n_{21}^2)\sin^2\omega - n_{21}^2}, \qquad K_2 = \frac{\sin^2\omega + n_{21}^2}{(1+n_{21}^2)\sin^2\omega - n_{21}^2} \quad (2)$$

and $C = (3n_{21}/2\cos\omega)N_{ref}d_p$ where $d_p = \lambda[2\pi(\sin^2\omega n^2_{ATR} - n^2_{sample})]^{-1}$ is the so-called penetration depth of electromagnetic waves.

The considered band represents the superposition of the absorbance of all absorbing groups. Hence, the total polarized absorbances are

$$A_{||} = \sum A_{||}^{ij} \quad \text{and} \quad A_\perp = \sum A_\perp^{ij} \quad (3)$$

where summation runs over all molecules and the absorbing groups ($\sum \equiv \sum_{i=1}^{n_{mol}} \sum_{j=1}^{n_{group}}$).

Let us introduce the dichroic ratio of a single group, $R^{ij} \equiv A_{||}^{ij}/A_\perp^{ij}$, and that of the sample:

$$R_{ATR} \equiv \frac{A_{||}}{A_\perp} = \frac{\sum R^{ij}A_\perp^{ij}}{\sum A_\perp^{ij}} = \frac{\sum R^{ij}(1 - S_{IR}^{ij})\epsilon^{ij}}{\sum (1 - S_{IR}^{ij})\epsilon^{ij}} \quad (4)$$

The observable R_{ATR} represents the mean value of the dichroic ratio of all absorbing groups in the sample weighted by the factor $(1 - S_{IR}^{ij})\epsilon^{ij}$. It yields the apparent IR order parameter of the absorption band

$$S_{IR} \equiv \frac{R_{ATR} - K_1}{R_{ATR} + K_2} \quad (5)$$

After insertion of eqs 1 and 4 into eq 5, one obtains

$$S_{IR} = \frac{\sum S_{IR}^{ij}\epsilon^{ij}}{\sum \epsilon^{ij}} \equiv \langle P_2(\theta_\mu)\rangle \quad (6)$$

The result shows that the IR dichroism experiment provides an absorption coefficient-weighted, ensemble-averaged second-order Lengendre polynomial of all groups in the sample which contribute to the considered absorption band.

Determination of Chain Order Parameters from IR Linear Dichroism Data. Let us introduce Cartesian $\{x^i, y^i, z^i\}$ coordinate systems that are fixed to the methylene groups of a polymethylene chain with axes x^i and y^i pointing along the bisectrice of the hydrogen−carbon−hydrogen bond angle of methylene groups $i = 1, ..., n_{group}$ and along the interconnecting line between both hydrogens, respectively. The z^i axes consequently orient along the interconnecting line between the midpoints of adjacent C−C bonds, and thus, a z^i axis defines the orientation of the local fiber axis of the chain. At first we consider a single chain, *j* (Figure 1, part A). Its mean long axis can be defined as the unit vector, $\mathbf{m}^j$, that points along the sum of unit vectors that are oriented along the segmental z^i axes. In a membrane, i.e., in an ensemble of chains, the chain axes fluctuate about the membrane director, **d**, which represents the mean orientation of all $\mathbf{m}^j$ (Figure 1, part B). The segmental ordering with respect to **d** can be characterized in terms of the diagonal elements of *Saupe's* order parameter matrix, $S_k \equiv S_{kk} = \langle P_2(\theta_k^{ij})\rangle_{arit}$, where θ_k^{ij} is the angle between **d** and axis $k = x^{ij}, y^{ij}, z^{ij}$ of segment *i* in chain *j*, and $\langle ...\rangle_{arit}$ denotes arithmetic averaging over all segments in the membrane.[30] The longitudinal order parameter

$$S_z = -(S_x + S_y) \quad (7)$$

is a measure of the conformational order of the chains. The so-called dispersion, $D_{xy} = S_x - S_y$, characterizes the transverse ordering perpendicular to the membrane director, i.e., within the membrane plane.[23,27] Fluid membranes typically lack transverse ordering ($D_{xy} = 0$).

Selective deuteration of the saturated acyl chains of the lipids allows evaluation of the molecular ordering of the stearoyl (SDPC-d35) and palmitoyl (POPC-d31) chains using the IR order parameters of the symmetric and antisymmetric CD_2 stretching bands near 2090 and 2195 cm^{-1}, $S_{IR}(\nu_s(CD_2))$ and $S_{IR}(\nu_{as}(CD_2))$, respectively.[27] In a first-order approximation, the respective transition moments are assumed to point along the segmental *x* and *y* axes, respectively. Hence, the IR linear dichroism of the methylene stretches yields the apparent longitudinal order parameter of the deuterated acyl chains in analogy to eq 7:

$$S_\theta(\text{stearoyl, palmitoyl}) \equiv -\{S_{IR}[\nu_s(CD_2)] + S_{IR}[\nu_{as}(CD_2)]\} \quad (8)$$

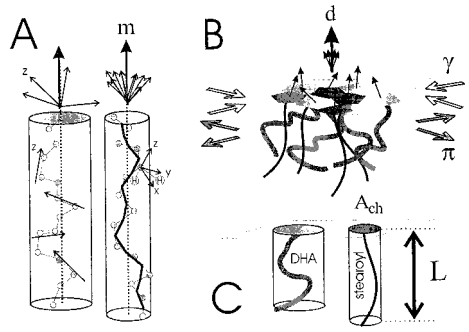

Figure 1. Schematic representation of a partially disordered polyunsaturated (left) and saturated (right) acyl chain in a membrane (part A), an ensemble of lipid chains in one-half of a bilayer (part B) and their mean projection length, *L*, and mean area requirement in the membrane plane, A_{ch} (part C). One methylene coordinate $\{x,y,z\}$ system is indicated in part A. The *z* axes define the fiber axes of the chains (thick line). The small arrows in part B illustrate fluctuating long axes of the chains. Their sum gives the local director, **d**. Note that A_{ch} defines an "effective" area that relates the mean projection length to the cross section area of a cylinder which does not necessarily reflect the real molecular shape of a chain. The symbol π denotes the repulsive lateral pressure which is counterbalanced by the cohesive hydrophobic surface tension, γ. Note, that the vertical offset distance between π and γ causes a bending stress within the bilayer. See text for details.

There exist, however, several factors that can cause a systematic difference between S_θ and S_z:

(i) S_θ represents a spectroscopic mean (see eq 6), whereas S_z is defined as an arithmetic average over all segments. In general, the absorption coefficient of the methylene stretches depends on substituents in the chain, such as carbonyl, methyl, or methine groups, and on the torsion angles of adjacent C−C bonds and, thus, on the conformation of the chain through changes in charge distribution.[31] One could suspect that ϵ^i decreases along the chain with increasing carbon number i because conformational disorder typically increases in lipid bilayers toward the methyl end groups.[32] It was however shown that the intensity of methylene stretches of alkanes and polyethylene decreases by less than 10% upon heating from 7 to 300 K.[31] In this temperature range the chains undergo a melting transition that is accompanied by considerable alterations of chain conformation. The observed intensity change could be mainly attributed to changes of the density and refractive index of the samples and only to a minor degree to a variation of the absorption coefficient. Moreover, the intensity of Raman spectra of dimyristoyl-PC specifically deuterated in the sn-2 chain at one of the positions $i = 3$, 4, 6, 10, 12, and 14 varies only slightly in the CD_2 stretching range.[33] We therefore assume that ϵ^i is a constant, and thus, the IR order parameters $S_{IR}(\nu_s(CD_2))$ and $S_{IR}(\nu_{as}(CD_2))$ and their sum S_θ can be interpreted as an arithmetic mean value of the segmental order parameters.

(ii) The orientation of the transition moments of the methylene stretches can slightly deviate from the expected perpendicular orientation relative to the fiber axis because of vibrational coupling along the chain.

(iii) Imperfect alignment of the membranes at the ATR surface, monolayer bending in nonlamellar phases, fluctuations of the local director due to undulations of the bilayers, and tilting of the chain axes can interfere with interpretation in terms of conformational ordering.[34−36]

Effects (ii) and (iii) can be considered in terms of a set of nested uniaxial order parameters if they act independently

$$S_{IR} \approx S_{\delta k} S_k S_d \quad \text{with} \quad k = x, y, z \tag{9}$$

The order parameters $S_{\delta k}$ and S_d are mean second-order Legendre polynomials of the angle between the transition moment, $\boldsymbol{\mu}$, and the respective coordinate axis and between the local director **d** and the ATR normal, **n**, respectively. Hence, the IR order parameters must be corrected according to eq 9 to yield the segmental order parameters of the deuterated chains:

$$S_z \approx S_\theta/(S_d S_{\delta z}) \tag{10}$$

The mean ordering of the protonated unsaturated chains of POPC-d31 and SDPC-d35 is also accessible in the IR linear dichroism experiment. The longitudinal order parameter of the polymethylene fragments of the oleoyl chains were determined from the IR order parameters of the symmetric and antisymmetric CH_2 stretches near 2852 and 2922 cm^{-1}, respectively:

$$S_\theta(\text{oleoyl}) \equiv -[S_{IR}(\nu_s(CH_2)) + S_{IR}(\nu_{as}(CH_2))] \tag{11}$$

The IR order parameter of the C−H bending mode of the −CH=CH− groups of the docosahexaenoyl chains at 1388 cm^{-1} yields the longitudinal order parameter of the polyunsaturated chain

$$S_\theta(\text{DHA}) \equiv S_{IR}(\delta(\text{C}-\text{H})) \tag{12}$$

This choice was motivated by the fact that $S_{IR}(\delta(C-H))$ reaches a maximum value near unity in the L_β phase of SDPC-d35 (vide infra). Consequently, the corresponding transition moments must point along the chain axis for symmetry reasons. A detailed discussion of the linear dichroism of SDPC will be given elsewhere.

Equation 10 in combination with eqs 8, 11, and 12 provides the longitudinal segmental order parameter of saturated and unsaturated acyl chains of SDPC-d35 and POPC-d31.

Determination of Mean Chain Dimensions from Order Parameters. In liquid-crystalline membranes, the mean projection length of the saturated sn-1 chain of lipids in direction of the membrane normal is approximately proportional to the segmental order parameter S_x.[32,37,38]

$$L \approx L_{max}(0.5 + |S_x|) \tag{13}$$

where L_{max} is the maximum chain length which corresponds to the extended all-trans conformation (see Figure 1, part C). Equation 13 was derived from a diamond lattice model of C−C bonds and ignores tumbling motions of the lipid, collective bilayer motions and chain upturns,[39] which have been observed experimentally[40] and in molecular dynamics simulations.[41] Despite of these simplifications, the analysis of ^2H NMR order parameters in terms of the diamond lattice model reflects bilayer dimensions in a satisfactory fashion, except for a slight overestimation of the area per lipid in comparison with X-ray data.[17] The origin of these differences is still debated (see refs 42 and 43 for details). According to previous experiments,[17] this discrepancy is of secondary importance for data analysis because eq 13 is applied to quantify the chain dimensions in a relative fashion, whereas X-ray data provide their absolute dimensions (see below).

Making use of eq 7 and of the condition of cylinder symmetry for rotations about the z axis, $S_x = S_y$, one obtains the chain length as a function of the longitudinal order parameter S_z:

$$L \approx 0.5 L_{max}(1 + S_z) \tag{14}$$

For incompressible acyl chains (volume per chain $v_{ch} \approx$ const.), one can write $v_{ch} \approx A_{min} L_{max} \approx A_{ch} L$ where A_{ch} and A_{min} denote the "effective" area requirement per chain in the membrane plane and its minimum value referring to $S_z = 1$, i.e., to the stretched chain. Insertion of eq 14 into $A_{ch} \approx A_{min} L_{max}/L$ provides an estimation of the area requirement per chain as a function of the longitudinal order parameter[37,39]

$$A_{ch} \approx 2A_{min}(1 + S_z)^{-1} \tag{15}$$

Note, that eq 15 gives an absolute measure of the area per chain in terms of order parameters where the minimum available area of a chain, A_{min}, is unknown per se. For an independent estimation one can assume equal minimum cross sections of saturated and monounsaturated chains in the sn-1 and sn-2 position of POPC-d31, $A_{min}(\text{sn-1}) \approx A_{min}(\text{sn-2})$. In experiments on PCs with a wide variety of acyl chains, Smaby et al.[44] showed that the minimum limiting area is nearly the same ($\sim$0.2 nm^2). Then, the ratio of chain areas

$$r = A_{ch}(\text{sn-1})/A_{ch}(\text{sn-2}) \approx (1 + S_z(\text{sn-2}))/(1 + S_z(\text{sn-1})) \tag{16}$$

provides the area fraction of the sn-1 chain as a function of chain order parameters:

$$f(\text{sn-1}) \equiv A_{ch}(\text{sn-1})/(A_{ch}(\text{sn-1}) + A_{ch}(\text{sn-2})) = r/(r+1) \quad (17)$$

Let us assume additivity of chain areas of the lipid, $A_L = A_{ch}(\text{sn-1}) + A_{ch}(\text{sn-2})$, which is justified if lipid hydrocarbon chains pack in a fluid, lattice-like structure. The total are per lipid determined by X-ray diffraction (eq 22, see below) can be split into areas of sn-1 and sn-2 chains using eq 17:

$$A_{ch}(\text{sn-1}) = f(\text{sn-1})A_L \quad \text{and} \quad A_{ch}(\text{sn-2}) = A_L - A_{ch}(\text{sn-1}) = (1 - f(\text{sn-1}))A_L \quad (18)$$

This method also allows comparison of the area per chain in different lipids using their order parameters. The cross section of the stearoyl chains of SDPC-d35, A_{ch}(stearoyl), can be related to the area of the palmitoyl chains of POPC-d31, A_{ch}(palmitoyl), if one assumes equal minimum chain areas of the saturated chains, A_{min}(stearoyl) $\approx A_{min}$(palmitoyl) (vide supra):

$$A_{ch}(\text{stearoyl}) = A_{ch}(\text{palmitoyl})(1 + S_z(\text{palmitoyl}))/(1 + S_z(\text{stearoyl})) \quad (19)$$

where A_{ch}(palmitoyl) $= A_{ch}$(sn-1) has been calculated by means of eq 18.

Hydration-Induced Deformation of Lipid Lamellae. The water activity (given in terms of relative humidity) in the sample chamber, $a_w \equiv$ RH/100%, was adjusted yielding a specific chemical potential of water

$$\Delta\mu_W \equiv \mu_W(a_W < 1) - \mu_W(a_W = 1) = k_B T \ln a_W \quad (20)$$

(k_B is the Boltzmann constant). The chemical potential of water is defined as its partial molar free energy, $\Delta\mu_W \equiv (\partial\Delta G/\partial R_{W/L})$ ($\Delta G = G(a_W < 1) - G(a_W = 1)$). The hydration-induced increment of the free energy can be divided into a contribution that accounts for lateral deformation of the membranes and a contribution that is related to changes of the water layer thickness between the membranes, d_W. Accordingly one can write the chemical potential of water in the form

$$\Delta\mu_W = \Delta\mu_W^{||} + \Delta\mu_W^{\perp}$$

with

$$\Delta\mu_W^{||} = (\partial\Delta G/\partial A_L)_{dw=const}\,(\partial A_L/\partial R_{W/L})$$

and

$$\Delta\mu_W^{\perp} = 0.5(\partial\Delta G/\partial d_W)_{AL=const}\,(\partial d_W/\partial R_{W/L}) \quad (21)$$

The mean area requirement per lipid in the membrane plane

$$A_L = 2V/d \quad (22)$$

was obtained by means of X-ray diffraction which provides the repeat distance, d. The volume

$$V \approx v_L + R_{W/L} v_W \quad (23)$$

was obtained by gravimetry which yields the number of water molecules per lipid, $R_{W/L}$.[20] The symbols v_L and v_W denote the molecular volumes of lipid and water, respectively. Approximation (23) holds for volumetrically incompressible lipid and water molecules. The mean thickness of the water gap in the multibilayer stacks

$$d_W = 2R_{W/L} v_W/A_L \quad (24)$$

was estimated assuming nonpenetrating water and lipid layers.[45] The limitation of this method is that it does not account for water-filled pockets that may form spontaneously in multilamellar dispersions of phosphatidylcholines at $R_{W/L} > 15$ resulting in a systematic overestimation of A_L.[17,42,46,47] In this work, such pockets can be ignored because experiments have been conducted at reduced hydration ($R_{W/L} < 15$).

The chemical potential of water, $\Delta\mu_W$, is directly related to the partial molecular volume of water, $\partial V/\partial R_{W/L} \approx v_W$:[17]

$$\Delta\mu_W = -\Pi\,(\partial V/\partial R_{W/L}) = -0.5\Pi\{d_W\,(\partial A_L/\partial R_{W/L}) + A_L\,(\partial d_W/\partial R_{W/L})\} \quad (25)$$

The isotropic hydration pressure is defined as $\Pi \equiv -\Delta\mu_W/v_W$. It can be approximated by an exponentially decaying function of water layer thickness, d_W:

$$\Pi \approx \Pi_0 \exp(-d_W/\lambda) \quad (26)$$

Comparison of eqs 21 and 25 provides the lateral compression pressure of one monolayer upon dehydration, i.e., the difference of lateral pressure between the partially hydrated and the fully hydrated "relaxed" layer:[16,17,19]

$$\Delta\pi \equiv -(\partial\Delta G/\partial A_L)_{dw=const} = |\pi(a_W < 1) - \pi(a_W = 1)| \approx 0.5 d_W \Pi \quad (27)$$

The lateral pressure at full hydration is conveniently set to γ_0, the interfacial tension of the hydrocarbon−water interface, $\pi(a_W = 1) \approx \gamma_0$. The apparent lateral compressibility modulus of a bilayer is defined as

$$K_A^{ap} \equiv -2A_L\,\partial\Delta\pi/\partial A_L \quad (28)$$

representing a measure of the resistance of a lipid layer to transverse compression. Equation 28 ignores contributions to area changes due to smoothing of thermal undulations of the lamellae which may have a significant effect on apparent area changes.[48] Making use of a correction term proposed by Rawicz et al.,[48] one can estimate the elastic modulus of direct compression, K_A, from its apparent value:

$$K_A = \{(K_A^{ap})^{-1} - (k_B T/16\pi k_c)\ln(\Delta\pi(2)/\Delta\pi(1))/(\Delta\pi(2) - \Delta\pi(1))\}^{-1} \quad (29)$$

The arguments "1" and "2" denote the respective pair of pressure data which give the local slope of the pressure/area isotherm (see below). The symbol k_c denotes the elastic bending modulus of the membrane.

The increase of the lateral pressure of lipid membranes upon lateral compression can be qualitatively interpreted within the framework of a simple polymer brush model of parallel chains (see ref 48 and references therein):

$$\Delta\pi = (N_{seg}A_{min}/A_{ch}^2) \times (3k_B T \ln(A_{min}/(A_{ch} - A_{min})) - u_{rot}) - \gamma_0 \quad (30)$$

The symbol u_{rot} represents the energy change upon rotation about one segmental bond to achieve a more bulky conformation. N_{seg} is the number of statistical segments per chain. For fluid lipid layers one can confidently apply $u_{rot} \approx 0$ and $\ln(A_{min}/(A_{ch} - A_{min})) \approx A_{min}/A_{ch}$ to obtain[48]

$$\Delta\pi \approx 3k_BTN_{seg}A_{min}^2/A_{ch}^3 - \gamma_0 \quad (31)$$

Equation 31 predicts direct proportionality between K_A and the lateral pressure (see eq 28):

$$K_A = 6(\Delta\pi + \gamma_0) \quad (32)$$

The reliability of eqs 31 and 32 was checked for lipid monolayers in the liquid-expanded state.[48]

Equation 31 applies to both chains of a mixed chain lipid, i.e., the same lateral pressure acts on both the sn-1 and sn-2 chain. The condition $\Delta\pi(\text{sn-1}) = \Delta\pi(\text{sn-2})$ yields

$$A_{ch}(\text{sn-1})/A_{ch}(\text{sn-2}) = \{N_{seg}(\text{sn-1})A_{min}(\text{sn-1})^2/N_{seg}(\text{sn-2})A_{min}(\text{sn-2})^2\}^{1/3} \quad (33)$$

Hence, the ratio of chain areas depends on the ratio of the number of statistical segments and minimum chain areas of the respective chains.

Hydration-Induced Variation of Chain Ordering at Constant Temperature. Equation 15 allows the estimation of the apparent isothermal expansion modulus of the chain area in multilamellar bilayer stacks from the RH-dependence of the longitudinal chain order parameter:

$$K_{aw}(\text{chain}) \equiv A_{ch}^{-1}\,\partial A_{ch}/\partial a_W|_{T=\text{const}} \approx -(1+S_z)^{-1}\,\partial S_z/\partial \text{RH} \times 100\% \quad (34)$$

Let us first consider the apparent isothermal expansion modulus of a lipid, $K_{aw}(\text{lipid}) \equiv A_L^{-1}\,dA_L/da_W|_{T=\text{const}} = A_L^{-1}\,(\partial A_L/\partial\pi)\text{-}(\partial\pi/\partial a_W)_{T=\text{const}} = -2/K_A\,(\partial\pi/\partial a_W)_{T=\text{const}}$ (see also eq 28 and assuming $K_A \approx K_A^{ap}$). Insertion of eqs 20 and 24 into eq 27 gives $\pi = -k_BT \ln a_W R_{W/L}/A_L + \gamma_0$. Derivation with respect to a_w yields $(\partial\pi/\partial a_W)_{T=\text{const}} = \Delta\pi\{-A_L^{-1}\,(\partial A_L/\partial a_W) + R_{W/L}^{-1}\,(\partial R_{W/L}/\partial a_W)\,|_{T=\text{const}} + (a_W|\ln a_W|)^{-1}\} + \partial\gamma_0/\partial a_W$, resulting after rearrangement in (see also eq 34):

$$K_{aw}(\text{lipid}) = \left(1 - \frac{2\Delta\pi}{K_A}\right)^{-1} \times \left[\frac{2}{K_A}\left\{\Delta\pi\left(\frac{1}{R_{W/L}}\frac{\partial R_{W/L}}{\partial a_W} + \frac{1}{a_W|\ln a_W|}\right) - \frac{\partial\gamma_0}{\partial a_W}\right\}_{T=\text{const}}\right] \quad (35)$$

Equation 35 also applies to each of both acyl chains of a mixed chain lipid because of mechanical equilibrium $\Delta\pi = \Delta\pi(\text{sn-1}) = \Delta\pi(\text{sn-2}) \approx -k_BT \ln a_W R_{W/L}/2A_{ch}$ (see eqs 24 and 27 with $A_L \approx 2A_{ch}$). Insertion into eq 35 yields

$$K_{aw}(\text{chain}) = \left(1 - \frac{2\Delta\pi}{K_A}\right)^{-1} \times \left[\frac{2}{K_A}\left\{\frac{k_BT}{2A_{ch}}\left(\left|\ln a_W\right|\frac{\partial R_{W/L}}{\partial a_W} + \frac{R_{W/L}}{a_W}\right) - \frac{\partial\gamma_0}{\partial a_W}\right\}_{T=\text{const}}\right] \quad (36)$$

For sake of simplicity, let us approximate the adsorption isotherm by a linear function, $R_{W/L} \approx R_{W/L}^{max}a_W$. The approximation is justified in the RH range 20%−70% (see isotherms of POPC and SDPC at 25 °C in ref 20). With $\gamma_0 =$ const. and $2\Delta\pi/K_A \ll 1$, one obtains

$$K_{aw}(\text{chain}) \approx +(k_BT/A_{ch})K_A^{-1}R_{W/L}^{max}(1 + |\ln a_W|) \quad (37)$$

It follows that the ratio of the apparent isothermal expansion moduli of the chains of a mixed chain lipid is inversely related to their compressibility moduli:

$$K_{aw}(\text{sn-1})/K_{aw}(\text{sn-2}) \approx K_A(\text{sn-2})/K_A(\text{sn-1}) \quad (38)$$

Temperature-Induced Variation of Chain Ordering at Constant Water Activity. The thermal expansion modulus of the chain area in multilamellar bilayer stacks at constant water activity is analogous to eq 34:

$$K_T(\text{chain}) \equiv A_{ch}^{-1}\,\partial A_{ch}/\partial T|_{a_W=\text{const}} \approx -(1+S_z)^{-1}\,\partial S_z/\partial T \times 100\% \quad (39)$$

The derivative of the area requirement per lipid with respect to temperature at constant water activity is $dA_L/dT|_{a_W=\text{const}} = (\partial A_L/\partial T)_{\pi=\text{const}} + (\partial A_L/\partial\pi)(\partial\pi/\partial T)_{a_W=\text{const}}$. The latter term considers the change of A_L owing to the temperature-induced variation of lateral pressure. The apparent expansion modulus of a lipid monolayer is defined as (see also eq 28 and assuming $K_A \approx K_A^{ap}$)

$$K_T(\text{lipid}) \equiv A_L^{-1}\,dA_L/dT|_{a_W=\text{const}} = A_L^{-1}\,(\partial A_L/\partial T)_{\pi=\text{const}} - 2/K_A\,(\partial\pi/\partial T)_{a_W=\text{const}} \quad (40)$$

Making use of eqs 20, 27, and 28, one obtains $(\partial\pi/\partial T)_{a_W=\text{const}} = \Delta\pi\{R_{W/L}^{-1}\,(\partial R_{W/L}/\partial T) - A_L^{-1}\,(\partial A_L/\partial T)|_{a_W=\text{const}} + T^{-1}\} + \partial\gamma_0/\partial T$, which gives

$$K_T(\text{lipid}) = \left(1 - \frac{2\Delta\pi}{K_A}\right)^{-1}\left[\frac{1}{A_L}\frac{\partial A_L}{\partial T}\bigg|_{\pi=\text{const}} - \frac{2}{K_A}\left\{\Delta\pi\left(\frac{1}{R_{W/L}}\frac{\partial R_{W/L}}{\partial T} + \frac{1}{T}\right) + \frac{\partial\gamma_0}{\partial T}\right\}_{a_W=\text{const}}\right] \quad (41)$$

Equation 41 also applies to lateral expansion of the chain areas because of the condition of mechanical equilibrium (vide supra). The temperature dependence of the interfacial tension in the temperature range 300 ± 30 K of an oil/water interface can be reasonably well approximated by a linear function:[49]

$$\gamma_0(T) \approx \gamma_0(T = T^*)(T/T^*) \quad \text{with} \quad T^* = 300\ \text{K} \quad (42)$$

With this approximation, eq 41 transforms for water activities near unity to

$$K_T(\text{chain}) \approx A_{ch}^{-1}\,\partial A_{ch}/\partial T|_{\pi=\text{const}} - 2\gamma_0(300\ \text{K})/(3K_A) \times 10^{-2} \quad (43)$$

The second term is a constant with an approximate value of 10^{-3} K^{-1}.

Results and Discussion

Ordering of the Saturated Chains and Bilayer Dimensions as a Function of Hydration. Figure 2 compares the mean vertical and lateral dimensions of the hydrophobic core of one-half of SDPC-d35 and POPC-d31 bilayers with the longitudinal order parameter and the mean CD_2 stretching frequency of the stearoyl and palmitoyl chains. The area per lipid, A_L and the mean chain length, L_{hc}, have been calculated from results of previous X-ray measurements[20] using the approach of nonpenetrating lipid/water layers[45] (see the Theory section and also the legend of Figure 2). The longitudinal chain order parameter, S_θ, and the center of gravity of IR absorption, $\text{COG}(\nu_s(CD_2))$, were obtained from IR investigations. The order parameter, S_θ, was calculated from the IR order parameters of the antisymmetric and symmetric methylene stretching bands of the

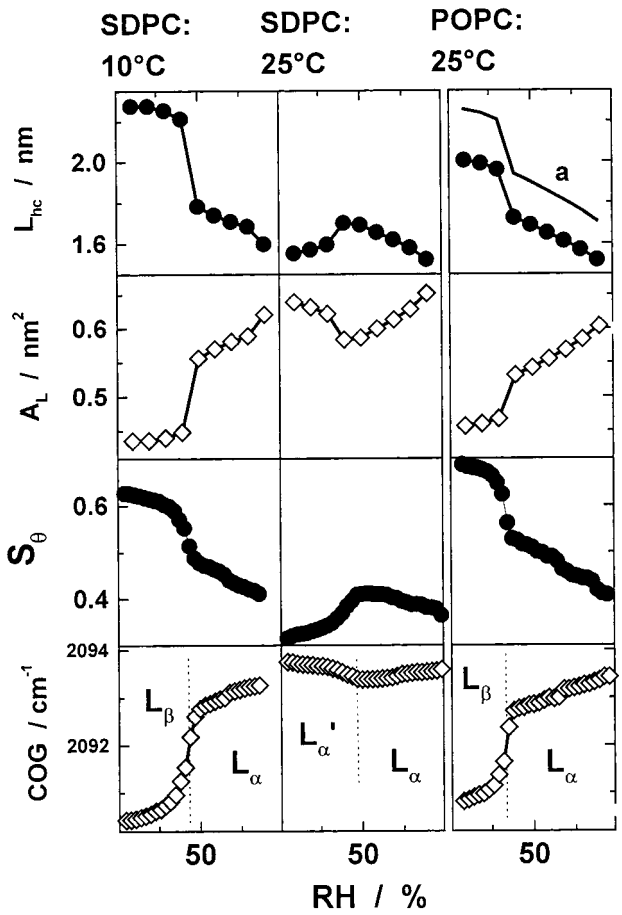

Figure 2. Bilayer dimensions and chain ordering of SDPC-d35 and POPC-d31 as a function of relative humidity (RH). Thickness of the hydrophobic core of one-half of the bilayer, L_{hc}; area per lipid, A_L; apparent chain order parameter of the saturated chain, S_θ (eq 8); and center of gravity of the symmetric CD_2 stretching band, COG($\nu_s(CD_2)$). Phase transitions are indicated by vertical dotted lines. $L_{hc} = 0.5d_{hc}$ was calculated using the repeat distance, d, with $d_{hc} = d - (d_{pol} + d_W)$ where d_W is the water layer thickness (eq 24) and $d_{pol} = 2\upsilon_{pol}/A_L$ is the thickness of the polar part of the bilayer. υ_{pol} denotes the volume of the nonhydrated polar part of the lipids which includes the glycerol and carbonyl moieties. For the PC lipids, we used the value $\upsilon_{pol} = 0.325$ nm^3 (see 41 and references therein). L_{hc} of POPC has been scaled with the factor $^{18}/_{16}$ to account for the different number of carbon atoms of the stearoyl and palmitoyl chains (graph a, see text). The respective diffractograms and repeat distances, d, were given previously.[20]

deuterated palmitoyl (POPC-d31) and stearoyl (SDPC-d35) chains by means of eqs 8 and 11, respectively.

The half-thickness of the hydrophobic core of POPC and SDPC bilayers in the gel phase, $L_{hc} \approx 1.98$ and 2.25 nm, respectively, slightly exceeds the length of the respective saturated chains in the all-trans conformation, $L_{max} \approx 1.91$ nm (palmitoyl) and 2.16 nm (stearoyl), that were estimated by means of $L_{max} \approx n_{CH_2}0.127$ nm (n_{CH_2} is the number of methylene groups per chain). Note that the difference of 0.06−0.09 nm between the calculated and measured values should be judged as the resolution limit of the model of nonpenetrating lipid/water layers owing to simplifying assumptions.[45] SDPC-d35 (10 °C) and POPC-d31 undergo a lyotropic chain melting transition from the gel (L_β) to the liquid-crystalline (L_α) phase with increasing RH. This event is characterized by a precipitous decrease of L_{hc} and S_θ, whereas A_L and COG($\nu_s(CD_2)$) markedly increase. Upon transformation into the L_α phase, the mean thickness and area of SDPC bilayers decrease by 20−25%, whereas L_{hc} and A_L of POPC membranes vary by less than 13% only. In contrast, the change of IR order parameters of the saturated chains in both lipids is similar (∼16% ± 3%).

Hydration of SDPC at 25 °C induces a transition between two lamellar fluid phases, L_α' and L_α, respectively. The L_α' bilayers exhibit the surprising tendency to contract laterally and to expand vertically with increasing RH, which is in contrast to L_α membranes that increase in area and decrease in thickness. For direct comparison with SDPC-d35, we scaled the L_{hc} values of POPC-d31 by a factor $^{18}/_{16}$ to take into account the different number of carbon atoms per saturated chain in both lipids (graph a in Figure 2). The comparison shows that increasing the number of double bonds in the sn-2 chain results in significantly thinner bilayers on a relative scale and in an increased area per lipid in the L_α phase at identical hydration. As a consequence, the hydrophobic half thickness of fluid membranes of the 18:0−22:6 lipid is similar to the value of the 16:0−18:1 lipid at $T =$ 25 °C (∼1.5 nm at RH > 95%).

Also, note the good correspondence between geometrical and IR parameters. Direct proportionality between the mean frequency of methylene stretches and the respective IR and ^{2}H NMR order parameters was previously reported for fluid lipid membranes.[50,51] Recently we found that the mean methylene stretching frequency of lipids with identical acyl chains in the sn-1 and sn-2 position is directly related to the mean area that the lipid molecules occupy in the membrane plane.[18] Hence, IR spectroscopy and X-ray diffraction independently provide information about hydration-induced changes of membrane dimensions.

It should be emphasized that X-ray diffraction yields an estimate of the mean geometry of both chains, whereas IR spectroscopy on the CD_2 stretches of sn-1 perdeuterated lipids selectively probes the saturated chains. Hence, subtle differences between the results of both methods possibly reflect different properties of the saturated and unsaturated chains of the mixed chain lipids. To explain the observed changes of bilayer dimensions, one might expect that the smaller variation of the order parameter of the stearoyl chains is related to a more pronounced change of the longitudinal ordering of the DHA chains at the chain melting transition of SDPC-d35. In contrast, the order parameter of the oleoyl and palmitoyl chains of POPC-d31 are expected to vary in a similar fashion because the changes in bilayer dimensions and in S_θ(palmitoyl) are almost equivalent.

Comparison between Order Parameters of Saturated and Unsaturated Chains. The degree of segmental ordering of the monounsaturated oleoyl chains of POPC-d31 was estimated in terms of the IR order parameters of the CH_2 stretches (eq 11), whereas order of the polyunsaturated DHA chains was obtained from the linear dichroism of the C−H wagging vibration of the methine groups (eq 12). Figure 2 compares the longitudinal order parameters S_z (eq 10) of the saturated and unsaturated chains of both lipids. The scaling factor in eq 10 was set to the maximum value of the respective chain order parameter in the L_β phase, $S_dS_{\delta z} = 0.75$ (stearoyl, palmitoyl, and oleoyl) and $S_dS_{\delta z} = 1$ (DHA), assuming stretched, nontilted chains (see ref 20). As expected, the order parameter of the DHA chains varies much more drastically (>40%) upon chain melting than the order of the stearoyl chains. Also the very similar drop of S_z of the oleoyl and palmitoyl chains confirms the expectation of equal changes in order of both chains for POPC-d31. These tendencies, i.e., a steeper slope of S_z of the polyunsaturated chain compared to the saturated and monounsaturated ones, were also observed in the fluid phases of SDPC-d35 and POPC-d31 (see legend of Figure 2). The order parameter of the stearoyl chain of SDPC-d35 decreases by a significantly smaller extent than the order

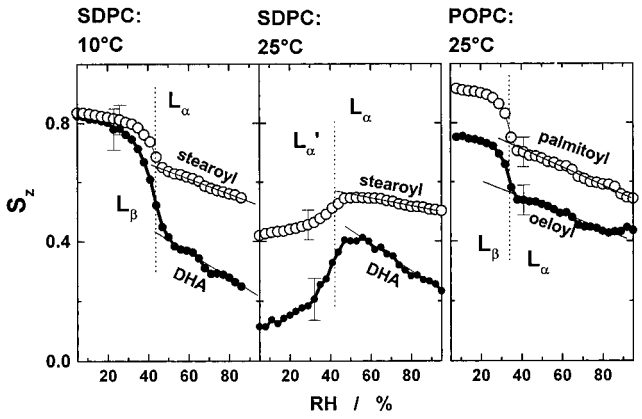

Figure 3. Longitudinal chain order parameters of SDPC-d35 and POPC-d31 as a function of relative humidity, RH. S_z was calculated by means of eqs 8, 11, 12, and 10 using $S_d S_{\delta z} = 0.75$ (methylene stretches) and 1.0 (C−H wagging vibration of DHA). The RH dependence of the order parameters was fitted by lines in the L_α phase. The slopes are 100% $\partial S_z/\partial \mathrm{RH} = -0.29 \pm 0.03$ (palmitoyl), -0.24 ± 0.03 (oeloyl), -0.22 and -0.14 (stearoyl chain at T = 10 °C and 25 °C, respectively), and -0.37 and -0.49 (DHA at T = 10 and 25 °C, respectively). Error is ±0.02.

parameter of the palmitoyl chain of POPC-d31 at 25 °C. Hence, both methods confirm independently that the dimensions and segmental ordering of polyunsaturated and monounsaturated chains in the mixed chain lipids change to a different degree as a function of hydration.

Equation 34 relates the variation of chain order parameters as a function of relative humidity to the relative change of chain area in the membrane plane. The ratio of the relative area change of the sn-1 and sn-2 chains is nearly a constants for each lipid in the whole RH range K_{aw}(sn-2)/K_{aw}(sn-1) = 1.0 (POPC-d31, 25 °C), 2.6, and 2.1 (SDPC-d35 at 25 °C and 10 °C, respectively; error ±0.5). This ratio is inversely related to the ratio of the isothermal compressibility moduli of the chains K_A-(sn-1)/K_A(sn-2) ≈ K_{aw}(sn-2)/K_{aw}(sn-1) (cf. eqs 35−38). Hence, the RH dependence of the chain order parameters suggests a smaller isothermal compressibility modulus of the DHA chains compared to stearoyl chains of SDPC-d35, whereas the palmitoyl and oleoyl chains of POPC-d31 are similarly compressible.

Dehydration-Induced Lateral Compression of the Membranes. Dehydration of lipid membranes is accompanied by a variation of lateral pressure. The correlation between the area per lipid, A_L, and the two-dimensional compression pressure, $\Delta\pi$ (eq 27), acting within the layer in the L_α phase, is shown in Figure 4. As expected, the lateral compression pressure increases with decreasing area due to steric repulsion between neighboring lipids. The simple polymer brush model provides a reasonable description of the experimental pressure−area isotherms in fluid membranes (see lines in Figure 4). The right shift of the SDPC isotherm (25 °C) with respect to the POPC isotherm indicates $N_{seg}{}^{05}A_{min}$(SDPC) > $N_{seg}{}^{05}A_{min}$(POPC) (see also eq 33), i.e., a bigger number of statistical segments and/or a bigger minimum area per chain for SDPC. The model parameters N_{seg} and A_{min} should be interpreted as mean values over both acyl chains of the mixed-chain lipids. In the next paragraph, we present a separate evaluation for each type of acyl chains.

The slope of the isotherms yields the apparent lateral area compressibility modulus, $K_A{}^{ap}$. Correction for the flattening of thermal undulation of the membranes using $k_c = 0.85 \times 10^{-19}$ J for POPC[48] (see eq 29) increases the elastic modulus of direct compression by less than 5% when compared with $K_A{}^{ap}$. Polyunsaturation was found to cause a distinct drop of k_c to

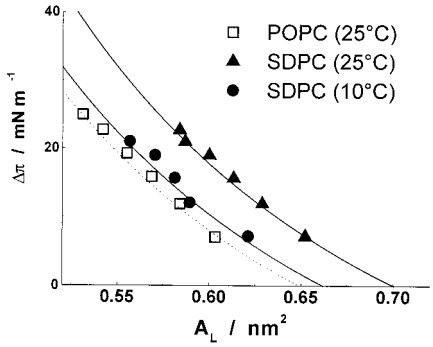

Figure 4. Lateral compression pressure, $\Delta\pi$, as a function of the area per lipid in the L_α phase of POPC and SDPC. The change of lateral pressure has been calculated by means of eq 27. The lines were calculated by means of eq 31 with $A_{ch} = 0.5A_L$, $\gamma_{phob} = 30$ mN/m, and $N_{seg}{}^{0.5}A_{min} = 0.29$ (POPC), 0.32 (SDPC, 25 °C), and 0.30 nm² (SDPC, 10 °C).

values near 0.4×10^{-19} J.[48] Eq 29 yields a correction to $K_A{}^{ap}$ of about +10%.

In the polymer brush model, K_A depends solely on $\Delta\pi$ and γ_0 (see eq 32). The assumed value of $\gamma_0 = 30$ mN/m agrees with the expected surface tension of the polar−apolar interface of 30−40 mN/m.[49] The respective isotherms refer to K_A = (180−330) mN/m for $\Delta\pi$ = 0−25 mN/m. The data reveal no significant difference between the area compressibility moduli of POPC and SDPC membranes in view of the relative error of ±20%. Within these error limits, our results agree also with recent micropipet pressurization measurements on giant vesicles of mono- and polyunsaturated lipids which yield an area dilation modulus of $K_A \approx 240$ mN/m.[48]

Lateral Compression of the Chains. The area of the mixed-chain lipid POPC-d31 was split into the mean cross sections of the palmitoyl and oleoyl chains by means of eqs 16−18 using the A_L data shown in Figure 2 in combination with the respective chain order parameters (Figure 3). The mean area per stearoyl chain of SDPC-d35 was estimated using eq 19, the order parameters of the saturated chains of SDPC-d35 and POPC-d31 (Figure 3), and the area per palmitoyl chain (Figure 5). Finally, the area requirement of the DHA chain of SDPC-d35 was calculated by eqs 16−18 in combination with the A_L data of SDPC-d35 (Figure 2). The results of this analysis are shown in Figure 5 as large symbols. For comparison, we also calculated the area per chain by eq 15 (small symbols in Figure 5) using a minimum value of $A_{min} = 0.2$ nm² for all chains which slightly exceeds the minimum cross section of a hydrocarbon chain in a paraffin crystal (∼0.19 nm²). The assumed minimum chain area is in agreement with the results of previous monolayer compression experiments ($A_{min} \approx 0.2$ nm² [44]). Furthermore, this value is in reasonable agreement with the area per lipid in the L_β phase of 0.43−0.45 nm² (SDPC) and 0.46−0.47 nm² (POPC, see Figure 2).

The similar $\Delta\pi - A_L$ data of the saturated chains of SDPC and POPC suggests that both membranes have similar hydrophobic surface tensions, γ_0 in the investigated hydration range. Note that a smaller surface tension in fully hydrated SDPC bilayers ($\Delta\pi = 0$) would increase the area per stearoyl chain compared to the palmitoyl chain in POPC. This would contradict the experimental results which indicated equal chain areas (uncertainty of A_L and γ_0: ∼10%). Therefore, isotherms according to the polymer brush model were calculated for the chains of POPC and SDPC individually using a common value of $\gamma_0 = 30$ mN/m (lines in Figure 5). A horizontal shift of an isotherm to larger areas is equivalent to an increase of the model

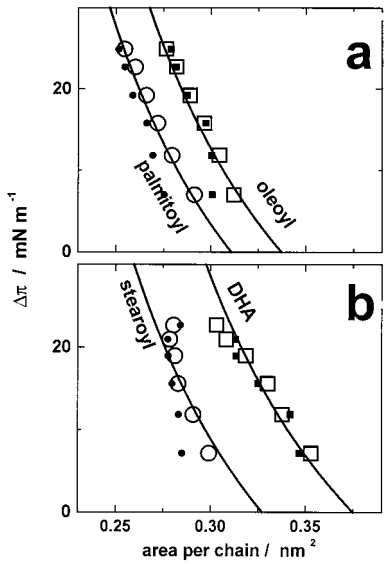

Figure 5. Lateral compression pressure, $\Delta\pi$, as a function of the mean area per oleoyl and palmitoyl chain of POPC-d31 (part a) and per DHA and stearoyl chain of SDPC-d35 (part b) at 25 °C. The data were calculated from X-ray and IR data by means of eqs 16−18 (large symbols, POPC-d31) and 19 (large symbols, SDPC-d35). The small symbols refer to an estimation using the S_z data shown in Figure 3 (eq 15) with $A_{min} = 0.2$ nm^2. The lines were calculated by means of eq 31 with $\gamma_{phob} = 30$ mN/m and $N_{seg}^{0.5}A_{min} = 0.27$ (palmitoyl), 0.305 (oleoyl), 0.29 (stearoyl), and 0.36 nm^2 (DHA).

parameter $N_{seg}^{0.5}A_{min}$ (see legend of Figure 5). With $A_{min} = 0.2$ nm^2 (vide supra), one obtains the number of statistical segments per chain, $N_{seg} = 1.8$ (palmitoyl), 2.1 (stearoyl), 2.3 (oleoyl), and 3.2 (DHA). A mean number of statistical segments of 2.25 was determined from the analysis of monolayer isotherms of SOPC at the water/air interface,[48] in good agreement with our estimate, $0.5(N_{seg}(\text{stearoyl}) + N_{seg}(\text{oleoyl})) = 2.20$.

However, the experimental isotherms of the stearoyl and DHA chains deviate in a systematic fashion from the calculated ones (Figure 5). In particular, at lateral pressures above 15 mN/m the experimental compressibility moduli are about 30% larger (stearoyl) or smaller (DHA) than the values predicted by the polymer brush model. The saturated chains are obviously less deformable by lateral pressure than the polyunsaturated ones. These data confirm also the results of our analysis of chain order parameters in terms of compressibility moduli given above. A qualitatively similar difference has been suggested for the compressibility moduli of DHA and stearoyl chains of SDPC at nearly full hydration ($a_W > 0.9$) comparing X-ray and ^{2}H NMR measurements.[17]

Flexibility of Saturated and Unsaturated Chains. Analysis in terms of the polymer brush model yielded an increased number of statistical segments of the mono- and polyunsaturated chains (at constant A_{min}) that increased their mean cross section compared to saturated chains. Normalization with respect to the number of C−C linkages per chain (including single and double bonds) provides the number of C−C linkages per statistical segment, $N_{cc} = (n_{carbons} - 1)/N_{seg} = 8.1 \pm 0.1$ for the saturated chains, N_{cc}(oleoyl) = 7.3 for the monounsaturated, and N_{cc}(DHA) = 6.6 for the polyunsaturated chains. Our value for the saturated chains agrees well with the effective segmental (Kuhn) length of short methylene polymers of $N_{cc} = 8.3$ (see 48 and references therein).

The decrease of N_{cc} with progressive unsaturation reflects increased flexibility. On first sight, this result is surprising because cis carbon−carbon double bonds represent rigid linkages about which rotation is energetically prohibited at room temperature. Consequently, the number of flexible hinges of a polyunsaturated chain is considerably smaller than the number of C−C bonds of a saturated chain with the same number of carbons. One could therefore expect N_{cc}(DHA) > N_{cc}(stearoyl) in contrast to our results. The smaller value of N_{cc}(DHA) shows that the smaller number of flexible C−C bonds of the DHA chains must be overcompensated by a higher degree of rotational freedom about the remaining C−C single bonds. The ═CH−CH$_2$− segments of the DHA chain preferentially exist in two energetically equivalent skew conformations with torsion angles ~±120° in contrast to the trans (180°) and gauche (±60°) conformations preferred by subsequent methylene segments of saturated chains.[52−54] These differences can cause sharper bends of the DHA chain axis and, thus, a shorter persistence length. Albrand et al.[55] calculated stable conformers of DHA chains which exist either in a stretched state or in a highly coiled conformation. Moreover, ab initio calculations on the flexibility of the two internal C−C bonds of 1,4-pentadiene indicate that the two rotors are virtually independent.[54] Consequently, the methylene bridges might introduce a high degree of flexibility in longer polyunsaturated chains. Details on the DHA conformations in membranes will be reported in a forthcoming publication.

Despite its crudeness, this simple approach confirms that unsaturation increases the flexibility and the lateral area requirement of the chains in lipid membranes. Note, that an increase of the minimum area per chain, A_{min}, at constant N_{seg} could explain an increase of chain area as well. In particular, it was reported that stretched oleoyl chains may occupy a slightly larger area accompanied by a smaller S_z than the palmitoyl chain due to a bend adjacent to the cis-C═C double bond which is suggested to cause a crankshaft kink motif to accommodate to the parallel alignment of the chain axes in the membrane.[52,56−58]

Thermodynamics of Bilayer Deformation. The incremental work of removing water from the bilayers goes into bilayer deformation and into work to overcome repulsive forces between apposing bilayers. The respective contributions to the chemical potential of water are given by eq 21. Figure 6 compares $\Delta\mu_W$ with the "potential of bilayer deformation", $\Delta\mu_W^{||}$, for SDPC at $T = 10$ and 25 °C and for POPC at $T = 25$ °C. Each phase transition is characterized by distinct extremum of $\Delta\mu_W^{||}$. Before and after the phase transitions, only a small fraction, typically less than 20% of the incremental free energy, goes into deformation. Hence, the dominant fraction of work to dehydrate the membranes is needed to decrease the distance between adjacent bilayers, in agreement with previous results.[16]

At the lyotropic chain melting transition of POPC, nearly the full amount of free energy that is released upon adsorption of water results from lateral expansion as indicated by the relation $\Delta\mu_W \approx \Delta\mu_W^{||}$. Consequently, no change of water layer thickness occurs. Note, that recent measurements by means of humidity titration calorimetry showed that the respective (exothermic) enthalpy of water adsorption roughly equals the (endothermic) heat of chain melting.[59] Upon chain melting of SDPC at 10 °C, we obtained $\Delta\mu_W > \Delta\mu_W^{||}$. This result implies that the exceeding amount, $\Delta\mu_W^{\perp} = \Delta\mu_W - \Delta\mu_W^{||}$, is consumed by the system to reduce the separation between the membranes.

At the $L_\alpha - L_\alpha'$ transition and in the L_α' phase of SDPC (25 °C), the sign of $\Delta\mu_W^{||}$ reverses compared to that of the L_α phase and becomes positive. That means, the system "redistributes" free energy from lateral into vertical deformation in addition to external work to dehydrate the lipids. The free energy that is released upon dehydration-induced lateral expansion goes into

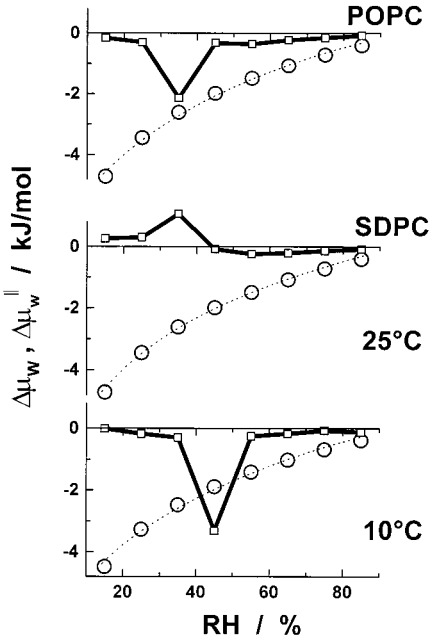

Figure 6. Chemical potential of water, $\Delta\mu_W$ (open circles), and the contribution of $\Delta\mu_W$ which goes into deformation of the membranes, $\Delta\mu_W^{\parallel} = -\Delta\pi\Delta A_L/\Delta R_{W/L}$ (small symbols, see eqs 21 and 27), as a function of relative humidity, RH.

the reduction of d_W. Recently, we showed that the $L_\alpha - L_\alpha'$ transition is driven by entropy.[20] Analysis in terms of vertical and horizontal contributions to $\Delta\mu_W$ shows that the respective gain of entropy at least partially results from lateral expansion of the bilayers.

Hydration Force. The increase of the isotropic hydration pressure, Π, is correlated with a decrease in thickness of the water gap between adjacent bilayers, d_W. Analysis in terms of an exponentially decaying function (eq 26) yields virtually equal decay lengths of the repulsive hydration force acting between SDPC and POPC membranes at 25 °C, $\lambda = 0.26 \pm 0.01$ nm (Figure 7). This result reflects the very similar hydration potency of both lipids.[20] However, it is important to note that the lateral compression pressure of POPC-d31 is bigger than that of SDPC-d35 at equal hydration pressure (see legend of Figure 7). Combining of eqs 26 and 27 yields

$$\Delta\pi(\mathrm{POPC}) - \Delta\pi(\mathrm{SDPC})|_{\Pi=\mathrm{const}} = 0.5\Pi\lambda \ln\{\Pi_0(\mathrm{POPC})/\Pi_0(\mathrm{SDPC})\} \approx 0.028\Pi$$

This difference corresponds to about 10% of the lateral compression pressure. The smaller contact pressure of SDPC-d35 may be related to a less compact packing of the headgroups compared with POPC-d31.[60]

The decay length of SDPC slightly increases to $\lambda = 0.30$ nm upon cooling to 10 °C. Separate analysis of solid (L_β) and fluid (L_α) membranes (see open and solid symbols in Figure 7) indicates virtually equal decay lengths λ in both phases for both lipids. The expected decrease of d_W at the chain melting transition of SDPC (vide supra) becomes evident as a horizontal shift of the respective ln $\Pi - d_W$ isotherms.

Temperature-Induced Variation of Chain Ordering. Figure 8 shows the temperature dependence of the chain order parameters, S_z, of POPC-d31 and SDPC-d35 films at humidity values RH < 100%. The $L_\beta - L_\alpha$ phase transition of POPC-d31 shifts to higher temperatures, T_m, with decreasing RH. The order parameters drops at the transition from about $S_z = 0.86$ to 0.70, independent of RH as long as RH ≥ 30%. Consequently, chain

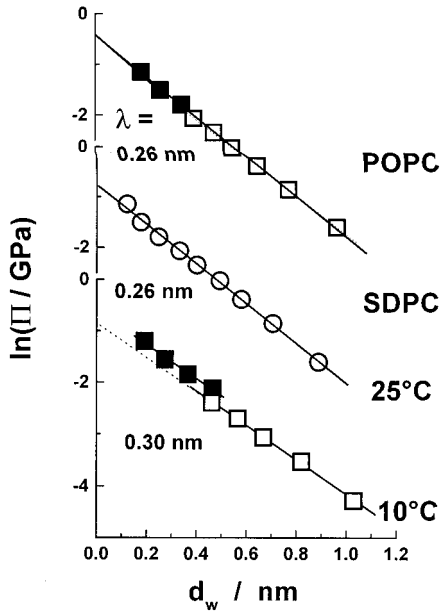

Figure 7. Semilogarithmic plots of the hydration pressure, Π, as a function of water layer thickness, d_W, of POPC (25 °C) and SDPC (25 °C and 10 °C; from top to bottom). Open and solid symbols refer to fluid and solid (L_β) membranes, respectively. Regression lines were calculated by means of eq 26. The respective decay lengths, λ, are reported within the figure (error ±0.01 nm). The contact pressures are $\Pi_0 = 0.6$ GPa for POPC and $\Pi_0 = 0.5$ GPa for SDPC (error ±0.05 GPa).

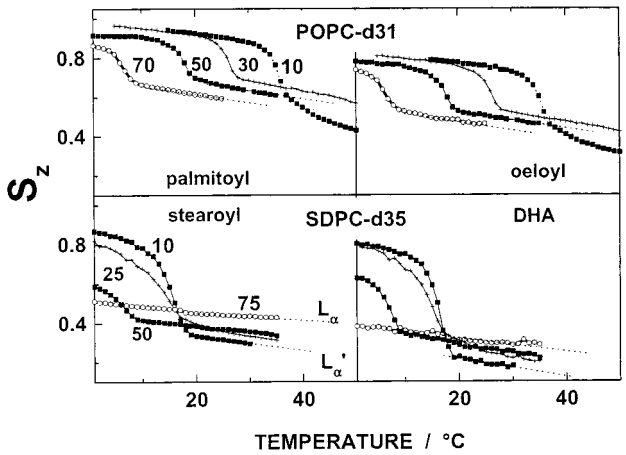

Figure 8. Chain order parameter S_z of POPC-d31 (above) and SDPC-d35 (below) hydrated at RH = const. (see figure for assignments; the numbers give RH in units of %) as a function of temperature. The order parameters were fitted by lines in the fluid phases of the lipids. The slopes are $\partial S_z/\partial T = -5.1 \pm 0.3$ (palmitoyl), -4.5 ± 0.3 (oleoyl), -1.5 and -2.9 (stearoyl chain at RH = 70% and 50%, respectively), -2.7 and -6.7 (DHA at RH = 70% and 50%, respectively), -5.3 and -4.0 (stearoyl at RH = 25% and 10%, respectively), and -8 and -6.7 (DHA at RH = 25% and 10%, respectively). All data are given in units of 10^{-3} K^{-1}. Error is ±0.5 if not stated otherwise.

ordering can be reasonably well described as a function of relative temperature, T/T_m. The more distinct decrease of S_z of nearly dry POPC-d31 (RH = 10%) at $T > 35$ °C is probably caused by the appearance of a nonlamellar phase.

In contrast to the behavior of POPC-d31, the transition temperature between the L_β and L_α' phases of SDPC-d35, at RH < 30%, is nearly independent of hydration. At RH > 30%, SDPC-d35 melts into the L_α phase. The temperature of this transition decreases with increasing RH, similar to the $L_\beta - L_\alpha$ transition of POPC-d31.

TABLE 1: Apparent Thermal Expansion Moduli, K_T,[a] of Acyl Chains of POPC-d31 and SDPC-d35 in Units of 10^{-3} K^{-1}

	POPC-d31		SDPC-d35	
phase	palmitoyl	oleoyl	stearoyl	DHA
L_α	3.6 ± 0.4	3.0 ± 0.4	0.9 ± 0.2 (RH = 75%)	1.6 ± 0.2 (RH = 75%)
			2.0 ± 0.2 (RH = 50%)	3.8 ± 0.3 (RH = 50%)
L_α'			3 ± 0.5	4 ± 0.5

[a] K_T was calculated by means of eq 39 using the slopes of the regression lines through the S_θ data shown in Figure 8.

The chain order parameter S_z of both lipids decreases almost linearly upon heating of the fluid phases (L_α and L_α'). Linear regression yields a similar slope, $\partial S_z/\partial T$, for the palmitoyl and oleoyl chains of POPC-d31 and for the stearoyl chains of SDPC-d35 in the L_α' phase (see legend of Figure 8). However, the order parameter of the DHA chains in the L_α' phase decreases more steeply than the order of the stearoyl chains. In the L_α phase, S_z(stearoyl) varies less with temperature than S_z(palmitoyl). The latter finding agrees with results of ^{2}H NMR measurements that reveal that chain ordering of the stearoyl chains of liquid-crystalline SDPC-d35 is less sensitive to temperature than chain ordering of sn-1 chain perdeuterated distearoyl PC and monounsaturated 1-stearoyl-2-oleoyl-PC.[21]

The slopes, $\partial S_z/\partial T$, and order parameters yield the apparent thermal expansion moduli (eqs 10 and 39) which are listed in Table 1. The measured K_T values fall into the typical range of thermal expansion moduli of liquid-crystalline lipid membranes of $1-5 \times 10^{-3}$ K^{-1}.[61] On one hand, the thermal expansion moduli of the polyunsaturated DHA chains are significantly bigger than those of the stearoyl chains, in particular in the L_α phase of SDPC-d35. On the other hand, the K_T values of both acyl chains of SDPC-d35 are smaller than the expansion moduli of the palmitoyl and oleoyl chains of POPC-d31 at RH $\geq$ 50%, K_T(oleoyl) $\approx$ K_T (palmitoyl) > K_T(DHA) > K_T(stearoyl), i.e., at conditions at which the first hydration shell of the lipids is completed.[20] We suggest that polyunsaturation decreases the sensitivity of the hydrophobic core of bilayers to temperature-induced changes of membrane dimensions compared to monounsaturated bilayers.

The polymer brush model (eq 31) predicts equal thermal expansion moduli for both chains of the mixed chain lipids because of $\Delta\pi$(sn-1) = $\Delta\pi$(sn-2). The condition K_T(sn-1) = K_T(sn-2) is approximately met for POPC-d31 but clearly fails for SDPC-d35. Equation 43 shows that the difference K_T(sn-2) $-$ K_T(sn-1) depends on the difference of the thermal expansion moduli of the chains at constant lateral pressure, $\{(A_{ch}(\text{sn-2})^{-1}\ \partial A_{ch}(\text{sn.2})/\partial T)_{\pi=\text{const}} - (A_{ch}(\text{sn-1})^{-1}\ \partial A_{ch}(\text{sn-1})/\partial T)_{\pi=\text{const}}\}$, and on $(K_A(\text{sn-1})^{-1} - K_A(\text{sn-2})^{-1})$, i.e., on the compression moduli of both chains. Hence, our result, K_T(DHA) > K_T(stearoyl), can be explained by a bigger thermal expansion modulus at π = const and/or by a bigger isothermal compression modulus of the DHA chains compared to that of the stearoyl chains. In other words, the DHA chains of the mixed chain lipid respond with higher sensitivity to thermal and/or mechanical perturbations of the membrane compared to saturated chains. The latter tendency was already derived from the results of the hydration studies (vide supra).

Temperature-Induced Changes in the Polar Region of the Membrane. Equation 40 shows that temperature affects chain dimensions "directly" via thermal excitation of conformational degrees of freedom and "indirectly" via variation of lateral pressure by a change of hydration of the polar part of the lipids and/or a change of surface tension, γ_0. Hence, the different response of chain ordering of monounsaturated POPC-d31 and of polyunsaturated SDPC-d35 to heating may reflect different hydration properties of both lipids. Details of lipid hydration can be studied by infrared spectroscopy.

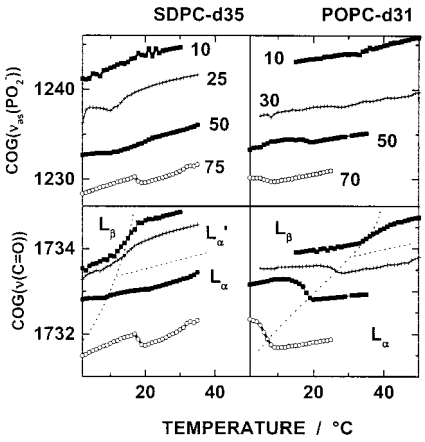

Figure 9. Local hydration characteristics of POPC-d31 (right) and SDPC-d35 (left) as a function of temperature at different values of relative humidity (see figure, the numbers indicate RH in units of %). Center of gravity of the antisymmetric phosphate stretching vibration, COG($\nu_{as}(PO_2^-)$) (above), and of the carbonyl stretching vibration, COG(ν(C=O)) (below). Phase boundaries are indicated by dotted lines (below).

We analyzed three hydration-sensitive IR parameters as a function of temperature (see Figure 9): (i) the center of gravity of the antisymmetric phosphate stretching mode, COG($\nu_{as}(PO_2^-)$), (ii) the center of gravity of the C=O stretching vibration, COG(ν(C=O)), and (iii) the integral absorbance of the O−H stretching band, $A(\nu_{13}(H_2O))$ (data not shown, see ref 62 for details). The latter parameter serves as a measure of the total amount of water that is sorbed to the lipid. The mean band positions, i and ii, characterize local hydration properties of specific water binding sites in the polar part of the bilayers because the respective absorption frequencies typically shift to smaller values upon progressive hydration as a result of H-bond formation between water and the phosphate-and carbonyl groups.[34,63−65]

The changes of the hydration sensitive parameters as a function of temperature are larger for SDPC-d35 than the changes for POPC-d31. Therefore, it is likely that polyunsaturation increases the sensitivity of lipid membranes to temperature-induced modifications in their polar region. According to eq 40, a positive slope of lateral pressure, $\partial\pi/\partial T > 0$, is expected to decrease the apparent area expansion modulus, K_T. Therefore, the difference K_T(SDPC) < K_T(POPC) may be caused by a stronger increase of lateral pressure in SDPC membranes upon heating. Indeed, the hydration-sensitive spectral parameters suggest that water binding to the polar moieties of SDPC weakens to a greater extent with temperature compared to POPC bilayers. Removal of water from the polar region is expected to reduce its volume and, thus, to give a positive contribution to lateral pressure. Consequently, the decreased sensitivity of the hydrophobic core of polyunsaturated bilayers to temperature at RH = const. could be at least partially explained by a temperature-induced increase of lateral pressure that counteracts the temperature-induced lateral expansion of the chains.

Thermotropic Phase Transitions and the Hydration of the Carbonyl Groups. The shift of the mean wavenumber of the ν(C=O) band at the phase transition reveals further differences

between mono- and polyunsaturated lipids. The C═O stretching frequency is known to be more sensitive to formation of H bonds with the carbonyl groups than to the conformation of the C−CO−O− fragments.[64] Consequently, the marked drop in wavelength of the COG(ν(C═O)) band at the $L_\beta-L_\alpha$ transition of POPC-d31 shows that the carbonyl groups become more accessible to H bonding upon chain melting.

In contrast, chain melting of SDPC-d35 (RH = 50%) has nearly no effect on the mean wavenumbers of the ν(C═O) band, and thus, hydration of the C═O moieties of the polyunsaturated lipid is probably not affected by this event. Interestingly, COG(ν(C═O)) even increases at RH < 50% where SDPC-d35 undergoes the $L_\beta-L_\alpha'$ phase transition. Water is obviously removed from the carbonyl region. This result surprises because the membranes laterally expand and one expects that a certain additional amount of water penetrates into the carbonyl region similar to the situation at the chain melting transition of POPC-d31. A partial dehydration of the carbonyl groups is characteristic for the transition of bilayers into a phase with inversely curved monolayers such as the inverse hexagonal or cubic phases.[34,63] Probably POPC-d31 undergoes such transition near $T \approx 35$ °C at RH = 10% (Figure 9). However, the L_α' phase of SDPC has all hallmarks of a lamellar phase as seen by X-ray diffraction and ^{31}P NMR.[20] A possible interpretation of the "peculiar" dehydration of the carbonyls in the L_α' phase of SDPC will be provided below.

In contrast to the ν(C═O) band, the hydration-sensitive parameters $A(\nu_{13}(H_2O))$ (not shown) and the mean wavenumber of the $\nu_{as}(PO_2^-)$ band remain virtually constant at the phase transition or vary smoothly in this region. This result lets us conclude that polyunsaturation predominantly modifies hydration properties and/or the conformational state of the carbonyl region but has little or no influence on hydration and/or conformation of the phosphate groups that are the primary hydration sites of phospholipids. Indeed, analysis of X-ray data in terms of hydration forces and gravimetric measurements[20] revealed very similar hydration potencies of both lipids at room temperature.

Polyunsaturation Changes the Profile of Lateral Pressure across the Bilayer. SDPC revealed the surprising property to expand laterally at the $L_\alpha-L_\alpha'$ phase transition and upon further dehydration in the L_α' phase. This tendency reflects an abnormal dehydration-induced decrease of hydrophobic surface tension that enables membrane area expansion. One could expect that modifications in hydration near the polar interface is correlated with a change of surface lateral pressure. Indeed, the abnormal alteration of membrane dimensions were paralleled by unusual changes of the spectral characteristics of the carbonyl groups that we interpreted as partial dehydration and/or a conformational change of these moieties. The deeper reason for the removal of water from the carbonyl region must be linked to the presence of polyunsaturated chains. Possibly the more polar character of the double bonds and/or the higher flexibility of the DHA chains promote partial dehydration of the carbonyl region. Indeed, the changes in saturated chain order parameters profile of fully hydrated SDPC-d35 as measured by ^{2}H NMR suggest that the center of weight of polyunsaturated chains is located closer to the lipid−water interface.[21] Furthermore, cross-relaxation rates from NOESY NMR experiments[66] and cross-polarization NMR spectroscopy[67] revealed temporary associations between molecular groups of the lipid/water interface and segments of the DHA chain. Therefore, it is possible that the polyunsaturated chain is slightly more exposed to the lipid-water interface region than the saturated chain, with apparent consequences for lipid hydration.

According to the concept of opposing forces, the cohesive interfacial tension is counterbalanced by the repulsive surface pressure, π, that is caused by repulsive forces between neighboring lipid molecules[68] (see Figure 1, part B). The lateral pressure acts across the whole thickness of the membrane, and thus, its profile, $p(z)$, is defined as the contribution of an infinitely thin layer at position z, where $z = 0$ is conveniently aligned to the polar interface near the carbonyls. Barotropic measurements showed that the C═O stretching frequency represents a sensitive marker of local compression in the carbonyl region of hydrated diacyl lipids.[69] We therefore suggest that the different behavior of the carbonyl groups of POPC-d31 and of SDPC-d35 at the thermotropic chain melting transition may also indicate differences in local pressure and, thus, of different pressure profiles in membranes of mono- and polyunsaturated lipids. Note that the high concentration of interfacial free energy within a narrow molecular region may result in enormous local pressures. For example, an increase of the lateral pressure by 5 mN/m within a layer with a thickness of 0.5 nm corresponds to a change of bulk pressure of 100 atm. Therefore, increased hydration of carbonyl groups may also be interpreted as a drop of local pressure that results in penetration of water into deeper interface regions, e.g., at the thermotropic chain melting transition of POPC. On the contrary, water is "squeezed out" at the thermotropic $L_\beta-L_\alpha'$ transition of SDPC because of increased local pressure that is acting on the carbonyls.

Polyunsaturated SDPC does not transform into a nonlamellar phase upon heating and/or dehydration contrary to the behavior of other phosphatidylcholines with monounsaturated and saturated hydrocarbon chains. The phase behavior of SDPC indicates a comparably small curvature stress upon dehydration. Curvature stress results from a vertical offset between the hydrophobic interfacial tension and the lateral pressure which effectively acts at the position which is given by the center of gravity of $p(z)$[49] (Figure 1, part B). Consequently, the absence of a lamellar-to-nonlamellar phase transition of SDPC reflects an altered pressure profile in membranes of polyunsaturated lipids.

Recently Cantor calculated profiles of lateral pressure for a series of saturated, cis-monounsaturated and cis-polyunsaturated hydrocarbon chains.[13] According to these calculations, multiple double bonds, as in DHA, are expected to shift the maximum of $p(z)$ toward the polar interface. Phase behavior of SDPC and the IR spectral characteristics of the C═O groups show that polyunsaturation may indeed increase the local pressure near the polar interface in accordance with the theoretical predictions. In any event, a change in the lateral pressure profile due to lipid polyunsaturation seems likely even if the shift of the COG(ν(C═O)) band may partly be the result of conformational changes near the carbonyl groups that are caused by polyunsaturation.

Summary and Conclusions

We conducted infrared linear dichroism and X-ray measurements to characterize the dimensions of lipid membranes as a function of hydration and temperature. The approach is based on the interpretation of mean segmental IR-order parameters of the acyl chains. Specificity for sn-1 and sn-2 chains was achieved by using mixed-chain lipids with perdeuterated, saturated hydrocarbon chains in position sn-1. Hydration studies provided information about resistance of chains to lateral compression. Furthermore, not only does hydration/dehydration

of lipid assemblies alter the amplitude of lateral pressure, but the related phase transitions are also a crude indicator for changes in the lateral pressure profile. The latter may be important for understanding the interaction of lipids with membrane proteins.

In mixed-chain polyunsaturated lipids, chain segmental ordering and chain dimensions of unsaturated and saturated chains are changing at different rates as a function of hydration. The DHA chains have a smaller isothermal compressibility modulus compared to the stearoyl chains of SDPC. The DHA chains of the mixed-chain lipid are more sensitive to external perturbations of the membrane than the saturated chains. In contrast, the palmitoyl and oleoyl chains of POPC have similar compressibility. The different properties of stearoyl and DHA chains may result in unfavorable chain packing upon dehydration that result in formation of a novel liquid-crystalline lamellar, L_α', phase with lower hydrocarbon chain order.[17,20] Analysis in terms of the polymer brush model shows that chain unsaturation increases the flexibility and mean area requirement of the chains in lipid membranes. The increased flexibility of the DHA chains is most likely the result of different conformers for rotations about $=CH-CH_2-$ bonds compared to rotations about $-CH_2-CH_2-$ bonds in saturated chains.

In the gel phase, the thickness of the hydrophobic core of SDPC bilayers exceeds the thickness of POPC bilayers because the chains adopt a stretched conformation in both lipids. Chain unsaturation causes fluid bilayers to thin on a relative scale. As a consequence, the effective hydrophobic thickness of fluid SDPC membranes with the longer 18:0 and 22:6 acyl chains is equal to the thickness of POPC membranes with the shorter 16:0−18:1 chains at room temperature. A constant hydrophobic thickness of the lipid bilayer may be important for lipid−protein interaction.

Temperature dependent measurements indicate that polyunsaturation decreases the sensitivity of the hydrophobic core of bilayers to temperature changes. This lack of sensitivity may be caused in part by a dehydration-induced increase of lateral pressure that counteracts the temperature-induced lateral expansion of the chains. Polyunsaturation predominantly modifies hydration properties of the carbonyl region but has little or no influence on hydration of the phosphate groups and of the whole lipid. Most likely, the higher flexibility of the polyunsaturated chain in combination with the polarizability of the double bonds are modifying water-binding to the carbonyls with consequences for interfacial tension.

Acknowledgment. This work was supported by the Deutsche Forschungsgemeinschaft within SFB 197 (TP A10).

References and Notes

(1) Brown, M. F. *Curr. Top. Membr.* **1997**, *44*, 285.
(2) Mitchell, D. C.; Gawrisch, K.; Litman, B. J.; Salem, N., Jr. *Biochem. Soc. Trans.* **1998**, *26*, 365.
(3) Kühlbrandt, W. *Nature* **2000**, *406*, 569.
(4) Jenski, L. J.; Nanda, P. K.; Jiricko, P.; Stillwell, W. *Biochim. Biophys. Acta* **2000**, *1467*, 293.
(5) Devaux, P. F.; Seigneuret, M. *Biochim. Biophys. Acta* **1985**, *822*.
(6) Bienvenüe, A.; Marie, J. S. *Curr. Top. Membr.* **1994**, *40*, 319.
(7) Caffrey, M.; Feigenson, G. W. *Biochemistry* **1981**, *20*, 1949.
(8) Baldwin, P. A.; Hubbell, W. L. *Biochemistry* **1985**, *24*, 2633.
(9) Kilian, J. A. *Biochim. Biophys. Acta* **1998**, *1376*, 401.
(10) Brown, M. *Chem. Phys. Lipids* **1994**, *73*, 159.
(11) Epand, R. M. *Biochim. Biophys. Acta* **1998**, *1376*, 353.
(12) Cantor, R. S. *J. Phys. Chem. B* **1997**, *101*, 1723.
(13) Cantor, R. S. *Biophys. J.* **1999**, *76*, 2625.
(14) Le Neveu, D. M.; Rand, R. P.; Parsegian, V. A. *Nature* **1976**, *259*, 601.
(15) Rand, P. *Annu. Rev. Biophys. Bioeng.* **1981**, *10*, 277.
(16) Parsegian, V. A.; Fuller, N.; Rand, R. P. *Proc. Natl. Acad. Sci. U.S.A.* **1979**, *76*, 2750.
(17) Koenig, B. W.; Strey, H. H.; Gawrisch, K. *Biophys. J.* **1997**, *73*, 1954.
(18) Binder, H.; Dietrich, U.; Schalke, M.; Pfeiffer, H. *Langmuir* **1999**, *15*, 4857.
(19) Evans, E. A.; Skalak, R. *Mechanics and thermodynamics of biomembranes*; CRC: Boca Raton, FL, 1980.
(20) Binder, H.; Gawrisch, K. *Biophys. J.* **2001**, *81*, *969*.
(21) Holte, L. L.; Peter, S. A.; Sinnwell, T. M.; Gawrisch, K. *Biophys. J.* **1995**, *68*, 2396.
(22) Schiller, J.; Arnhold, J.; Bernard, S.; Müller, M.; Reichl, S.; Arnold, K. *Anal. Biochem.* **1998**, *267*, 46.
(23) Binder, H. *Vib. Spectrosc.* **1999**, *21*, 151.
(24) Katsaras, J. *Biophys. J.* **1998**, *75*, 2157.
(25) Naumann, C.; Brumm, T.; Bayerl, T. M. *Biophys. J.* **1992**, *63*, 1314.
(26) Binder, H.; Anikin, A.; Kohlstrunk, B.; Klose, G. *J. Phys. Chem. B* **1997**, *101*, 6618.
(27) Binder, H.; Schmiedel, H. *Vib. Spectrosc.* **1999**, *21*, 51.
(28) Kota, Z.; Debreczeny, M.; Szalontai, B. *Biospectroscopy* **1999**, *5*, 169.
(29) Harrick, N. J. *Internal Reflection Spectroscopy*; Wiley: New York, 1967.
(30) Saupe, A. *Z. Naturf.* **1964**, *A 19*, 161.
(31) Snyder, R. G.; Maroncelli, M.; Strauss, H. L.; Hallmark, V. M. *J. Phys. Chem.* **1986**, *90*, 5623.
(32) Seelig, A.; Seelig, J. *Biochemistry* **1974**, *13*, 4839.
(33) Bansil, R. J.; Day, J.; Meadows, M.; Rice, D.; Oldfield, D. *Biochemistry* **1980**, *19*, 1938.
(34) Binder, H.; Anikin, A.; Lantzsch, G.; Klose, G. *J. Phys. Chem. B* **1999**, *103*, 461.
(35) Binder, H.; Pohle, W. *J. Phys. Chem. B* **2000**, *104*, 12039.
(36) May, S.; Ben-Shaul, A. *Biophys. J.* **1999**, *76*, 751.
(37) Schindler, H.; Seelig, J. *Biochemistry* **1975**, *14*, 2283.
(38) Bloom, M.; Evans, E.; Mouritsen, O. G. *Quart. Rev. Biophys.* **1991**, *24*, 293.
(39) Nagle, J. F. *Biophys. J.* **1993**, *64*, 1476.
(40) Huster, D.; Gawrisch, K. *J. Am. Chem. Soc.* **1999**, *121*, 1992.
(41) Feller, S. E.; Huster, D.; Gawrisch, K. *J. Am. Chem. Soc.* **1999**, *121*, 8963.
(42) Nagle, J. F.; Tristam-Nagle, S. *Biochim. Biophys. Acta* **2000**, *1469*, 159.
(43) Petrache, H. I.; Dodd, S. W.; Brown, M. F. *Biophys. J.* **2000**, *79*, 3172.
(44) Smaby, J. M.; Muderhwa, J. M.; Brockman, H. L. *Biochemistry* **1994**, *33*, 1915.
(45) Luzzati, V. *X-ray diffraction studies of lipid-water systems*; Academic Press: London, 1968; Vol. 1.
(46) Gawrisch, K.; Richter, W.; Möps, A.; Balgavy, P.; Arnold, K.; Klose, G. *Stud. Biophys.* **1985**, *108*, 5.
(47) Klose, G.; König, B.; Meyer, H. W.; Schulze, G.; Degovics, G. *Chem. Phys. Lipids* **1988**, *47*, 225.
(48) Rawicz, W.; Olbrich, K. C.; McIntosh, T.; Needham, D.; Evans, E. *Biophys. J.* **2000**, *79*, 328.
(49) Marsh, D. *Biochim. Biophys. Acta* **1996**, *1286*, 183.
(50) Le Bihan, T.; Pezolet, M. *Chem. Phys. Lipids* **1998**, *94*, 13.
(51) Kodati, V. R.; Lafleur, M. *Biophys. J.* **1993**, *64*, 163.
(52) Li, S.; Lin, H.-N.; Wang, Z.-Q.; Huang, C. *Biophys. J.* **1994**, *66*, 2005.
(53) Applegate, K. R.; Glomset, J. A. *J. Lipid Res.* **1986**, *27*, 658.
(54) Schurink, T. M.; DeJong, S. *Chem. Phys. Lipids* **1977**, *19*, 313.
(55) Albrand, M.; Pageaux, J.-F.; Lagarde, M.; Dolmazon, R. *Chem. Phys. Lipids* **1994**, *72*, 7.
(56) Siminovitch, D. J.; Wong, P. T. T.; Berchtold, R.; Mantsch, H. H. *Chem. Phys. Lipids* **1988**, *46*, 79.
(57) Pace, R. J.; Chan, S. I. *J. Chem. Phys.* **1982**, *76*, 4217.
(58) Klose, G.; Levine, Y. L. *Langmuir* **1999**, *16*, 671.
(59) Binder, H.; Kohlstrunk, B.; Heerklotz, H. H. *J. Colloid Interface Sci.* **1999**, *220*, 235.
(60) Binder, H.; Gutberlet, T.; Anikin, A.; Klose, G. *Biophys. J.* **1998**, *74*, 1908.
(61) Kwok, R.; Evans, E. A. *Biophys. J.* **1981**, *35*, 637.
(62) Binder, H.; Arnold, K.; Ulrich, A. S.; Zschörnig, O. *Biophys. Chem.* **2001**, *90*, 57.
(63) Castresana, J.; Nieva, J.-L.; Rivas, E.; Alonso, A. *Biochem. J.* **1992**, *282*, 467.
(64) Blume, A.; Hübner, W.; Messner, G. *Biochemistry* **1988**, *27*, 8239.
(65) Pohle, W.; Selle, C.; Fritzsche, H.; Binder, H. *Biospectroscopy* **1998**, *4*, 267.
(66) Huster, D.; Arnold, K.; Gawrisch, K. *Biochemistry* **1998**, *37*, 17299.
(67) Everts, S.; Davis, J. H. *Biophys. J.* **2000**, *79*.
(68) Tanford, C. *The hydrophobic effect*; Wiley and Sons: New York, 1973.
(69) Wong, P. T. T.; Siminovitch, D. J.; Mantsch, H. H. *Biochim. Biophys. Acta* **1988**, *947*, 139.